Contact Damage of Brittle Solids

B.R. Lawn

Solid-Solid Interactions. Proceedings of the First Royal Society—Unilever Indo-UK Forum in Materials Science and Engineering, M.J. Adams, B.J. Briscoe and S.K. Biswas, eds. Imperial College Press—Royal Society of London, London, p.29, 1995.

CONTACT DAMAGE OF BRITTLE SOLIDS

Brian Lawn
Materials Science and Engineering Laboratory
National Institute of Standards and Technology
Gaithersburg, MD 20899, U.S.A.

Abstract

A new kind of irreversible deformation in otherwise brittle solids has been observed in Hertzian contacts. The deformation takes the form of a distributed damage zone below the contact circle, instead of the conventional Hertzian cone fracture outside. An important manifestation of the damage is an effective "quasi-ductility" in the indentation stress–strain response. Control of the associated brittle–ductile transition is effected by incorporation of weak interfaces, large and elongate grains, and high internal stresses in the ceramic microstructure. Routes to micromechanical models of these processes, and ensuing implications concerning the prospective design of advanced flaw-tolerant and fatigue- and wear-resistant brittle materials, will be discussed.

Key Words

Brittle solids, contact fatigue, Hertzian contact, microstructure, quasi-ductile damage

1. Brittle Solids and Toughness

Brittle solids, notably ceramics, are limited in their structural usefulness by their lack of toughness [1]. Of the various mechanisms proposed to increase toughness in polycrystalline ceramics, "grain bridging" is the most effective and widespread [2-13]. In this process, frictional pullout of interlocking grains and second-phase particles in the crack-tip wake retards crack-wall separation. The retarding effect of the bridges increases until the interlocking grains disengage behind the crack tip, so that the toughness increases monotonically to a long-crack plateau. This increasing toughness describes the so-called "toughness curve" (*T*-curve or *R*-curve).

There are certain elements of the ceramic microstructure that enhance the effectiveness of bridging, and these have been incorporated into toughness models [4,8]. This has led to microstructural design prescriptions for enhanced long-crack toughness: (a) incorporate weak grain or interphase boundaries, to promote crack deflection and thus promote grain interlock; (b) include large (or elongate) grains or particles, to maximise interlock pullout distance; (c) maximise internal stress mismatch (e.g. from thermal expansion anisotropy), to clamp the interlocking grains in compression. However, the last element can have countervailing deleterious effects in the short-crack region by introducing local *tensile* stresses at some grain facets, thereby promoting local microfracture [1,8]. The implication is that enhancement of traditional long-crack toughness can have deleterious effects in the short-crack region, where wear, erosion, and contact fatigue properties are determined.

2. Hertzian Test

We address this last issue by using the Hertzian test configuration in figure 1, in which a hard sphere of radius r is loaded onto a flat specimen surface. The rationale for using this particular test is that the Hertzian field contains a strong component of compression, so that large-scale fractures can be largely suppressed in favour of microscale events. From the load P and contact radius a one may plot indentation stress $p_0 = P/\pi a^2$ versus indentation strain a/r to

produce an indentation stress–strain curve [14-16]. In our experiments, a special specimen configuration, consisting of two polished rectangular half-blocks bonded together with thin adhesive, allows us to obtain section as well as surface views of the contact damage [14]. Indentations are placed symmetrically across the trace of the bonded interface on the top surface. After indentation, the adhesive is dissolved and the half-blocks separated to reveal the subsurface damage in section view. The top and side surfaces of the half-blocks are then coated with gold, and viewed in Nomarski illumination.

In conventional homogeneous, low toughness materials like glass, single crystals, and fine-grain polycrystals, the Hertzian test produces a classical cone crack outside the contact, where modest tensile stresses exist [17-22]. In heterogeneous, high toughness materials, however, we find something altogether different; namely, a distributed damage zone below the contact, where the stresses are high in compression but also in shear [14,15,23-27]. We illustrate here with two silicon carbide ceramics, differing only in microstructural heterogeneity [25]. Figure 2a shows half-surface and subsurface patterns for a fine-grain material with strong grain boundaries and weak internal stresses. Figure 2b shows comparative views for a material with coarsened and elongated platelet grains bonded by a second phase, and weak, highly stressed interphase boundaries. The indentation stress–strain curve for the heterogeneous material shows a relatively enhanced nonlinearity, more reminiscent of a ductile metal [24,25].

A major advantage of the Hertzian test, apart from its simplicity, is its capacity for extension to cyclic fatigue analysis [14,28,29]. Microscopic examination of the heterogeneous silicon carbide in figure 2b after repeat loading to a fixed peak load reveals progressive degradation of the material, with ultimate interphase boundary breakdown and formation of debris [29]. By contrast, the homogeneous material in figure 2a shows much less susceptibility to damage accumulation. Material removal is thereby enhanced by the microstructural heterogeneity. Whereas this enhanced removal rate increases the susceptibility to wear [26,30,31], it also raises the attractive prospect of a machinable silicon carbide ceramic [32]. Further, since the subsurface damage does not propagate as a single deep crack, the attendant strength loss associated with the incidence of contact damage is much reduced, thus improving the flaw tolerance [32].

Scanning electron microscopy reveals that the subsurface damage seen in figure 2b arises from the action of microfailures at the weak interfaces in the heterogeneous silicon carbide [32,33]. These microfailures are activated by shear stresses, and are hence referred to as "shear faults". Key to containment of the damage accumulation is microstructural discreteness, to allow individual shear faults to evolve independently without catastrophic failure, and frictional sliding at the fault interfaces, to dissipate mechanical energy [33].

3. Models and Future Work

Models are being constructed to describe the observations [16]. The deformation of a single shear fault element is shown in figure 3a for a platelet structure. Deformation is constrained by friction at the sliding interfaces and by the confining elastic matrix at the ends of the platelet. One begins by determining a constitutive relation between the contact pressure (which determines the intensity of the stress field) and the shear strain (governed by the platelet geometry) for the element. Integration over all such elements within the contact deformation volume, figure 3b, allows one to derive an expression for the indentation stress–strain response in terms of microstructural variables, e.g. platelet volume fraction, size l, aspect ratio, l/w, and friction coefficients. In some materials like alumina [14,23] and silicon nitride [26], the stress concentrations that manifest themselves at the fault ends can generate highly localised, stable microcracks which can extend on unloading and ultimately coalesce, enhancing the damage still further [34].

Work on this kind of damage accumulation in a range of brittle ceramics (alumina, glass-ceramics, zirconia, silicon nitride) is being continued in our laboratories. Various techniques (acoustic emission, thermal wave imaging, transmission electron microscopy) are being employed to characterise the damage, and theoretical models developed to quantify the microstructural variables. It is hoped that these studies will provide useful design guidelines for developing the next generation of high-strength, wear- and fatigue-resistant, materials.

Acknowledgements

The micrographs in figure 2 were kindly provided by N.P. Padture. The author acknowledges contributions from the following colleagues at NIST: H. Cai, F. Guiberteau, N.P. Padture, A. Pajares, H. Xu, L. Wei. Funding was provided by the U.S. Air Force Office of Scientific Research.

References

1. B.R. Lawn, *Fracture of Brittle Solids*, Second, Cambridge University Press, Cambridge (1993).
2. C.J. Fairbanks, B.R. Lawn, R.F. Cook and Y.-W. Mai, *Fracture Mechanics of Ceramics*, (edited by R.C. Bradt, A.G. Evans, D.P.H. Hasselman and F.F. Lange), Vol. 8, p. 23. Plenum, New York, (1986).
3. P.L. Swanson, C.J. Fairbanks, B.R. Lawn, Y.-W. Mai and B.J. Hockey, *J. Am. Ceram. Soc.* **70,** 279 (1987).
4. Y.-W. Mai and B.R. Lawn, *J. Am. Ceram. Soc.* **70,** 289 (1987).
5. R.W. Steinbrech, A. Reichl, F. Deuerler and W. Schaarwachter, *Science of Ceramics* **14,** 659 (1987).
6. P.L. Swanson, *Fractography of Glasses and Ceramics*, (edited by J. Varner and V.D. Frechette), Vol. 22, p. 135. American Ceramic Society, Columbus, OH, (1988).
7. M. Sakai and R.C. Bradt, *Nippon-Seramikkusu-Kyokai-Gakujutsu-Ronbunshi* **96,** 801 (1988).
8. S.J. Bennison and B.R. Lawn, *Acta Metall.* **37,** 2659 (1989).
9. E.K. Beauchamp and S.L. Monroe, *J. Am. Ceram. Soc.* **72,** 1179 (1989).
10. J. Rödel, J. Kelly and B.R. Lawn, *J. Am. Ceram. Soc.* **73,** 3313 (1990).
11. P. Chantikul, S.J. Bennison and B.R. Lawn, *J. Am. Ceram. Soc.* **73,** 2419 (1990).
12. G. Vekinis, M.F. Ashby and P.W.R. Beaumont, *Acta Metall.* **38,** 1151 (1990).
13. K.W. White and G.P. Kelkar, *J. Am. Ceram. Soc.* **74,** 1732 (1991).
14. F. Guiberteau, N.P. Padture, H. Cai and B.R. Lawn, *Philos. Mag.* **A 68,** 1003 (1993).
15. H. Cai, M.A. Stevens Kalceff and B.R. Lawn, *J. Mater. Res.* **9,** 762 (1994).
16. A.C. Fischer-Cripps and B.R. Lawn, *Acta Metall.* **44,** 519 (1996).
17. H. Hertz, *Hertz's Miscellaneous Papers*, Macmillan, London, Chs. 5,6 (1896).
18. F.C. Roesler, *Proc. Phys. Soc. Lond.* **B69,** 981 (1956).
19. F.C. Frank and B.R. Lawn, *Proc. Roy. Soc. Lond.* **A299,** 291 (1967).
20. F.B. Langitan and B.R. Lawn, *J. Appl. Phys.* **40,** 4009 (1969).

21. T.R. Wilshaw, *J. Phys. D: Appl. Phys.* **4,** 1567 (1971).

22. B.R. Lawn and T.R. Wilshaw, *J. Mater. Sci.* **10,** 1049 (1975).

23. F. Guiberteau, N.P. Padture and B.R. Lawn, *J. Am. Ceram. Soc.* **77,** 1825 (1994).

24. B.R. Lawn, N.P. Padture, H. Cai and F. Guiberteau, *Science* **263,** 1114 (1994).

25. N.P. Padture and B.R. Lawn, *J. Am. Ceram. Soc.* **77,** 2518 (1994).

26. H.H.K. Xu, L. Wei, N.P. Padture, B.R. Lawn and R.L. Yeckley, *J. Mater. Sci.* **30,** 869 (1995).

27. A. Pajares, F. Guiberteau, B.R. Lawn and S. Lathabai, *J. Am. Ceram. Soc.* **78,** 1083 (1995).

28. H. Cai, M.A.S. Kalceff, B.M. Hooks, B.R. Lawn and K. Chyung, *J. Mater. Res.* **9,** 2654 (1994).

29. N.P. Padture and B.R. Lawn, *J. Am. Ceram. Soc.* **78,** 1431 (1995).

30. H.H.K. Xu and S. Jahanmir, *J. Am. Ceram. Soc.* **77,** 1388 (1994).

31. H.H.K. Xu, N.P. Padture and S. Jahanmir, *J. Am. Ceram. Soc.* **78,** 2443 (1995).

32. N.P. Padture, C.J. Evans, H.H.K. Xu and B.R. Lawn, *J. Am. Ceram. Soc.* **78,** 215 (1995).

33. N.P. Padture and B.R. Lawn, *Acta Metall.* **43,** 1609 (1995).

34. B.R. Lawn, N.P. Padture, F. Guiberteau and H. Cai, *Acta Metall.* **42,** 1683 (1994).

35. B.R. Lawn, *Journal of the European Ceramic Society* **7,** 17 (1991).

36. D. Tabor, *Hardness of Metals*, Clarendon, Oxford (1951).

37. K.E. Puttick, *J. Phys. D: Appl. Phys.* **12,** L19 (1979).

38. B.R. Lawn and D.B. Marshall, *J. Am. Ceram. Soc.* **62,** 347 (1979).

Figure captions

1. Hertzian test geometry, for bonded-interface specimen. Sphere, radius, r, delivers load P over contact radius a. Specimen consists of two polished halves glued together across symmetry interface.
2. Half-surface (upper) and section (lower) views of Hertzian contact damage in SiC, using tungsten carbide sphere of radius 3.18 mm at load 2000 N: (a) homogeneous fine-grain form, showing cone crack; (b) heterogeneous coarse-grain form, showing distributed subsurface damage. Optical Nomarski interference illumination.
3. Shear fault model for platelet structure. (a) Deformation of platelet of length l and thickness w within matrix, by sliding at upper and lower interfaces under action of net shear stress (heavy arrows). Sliding is constrained within elastic matrix, by resistive pressure at ends (light arrows). (b) Volume element containing distribution of platelets in contact stress field, subject to principal compression stresses (heavy arrows).

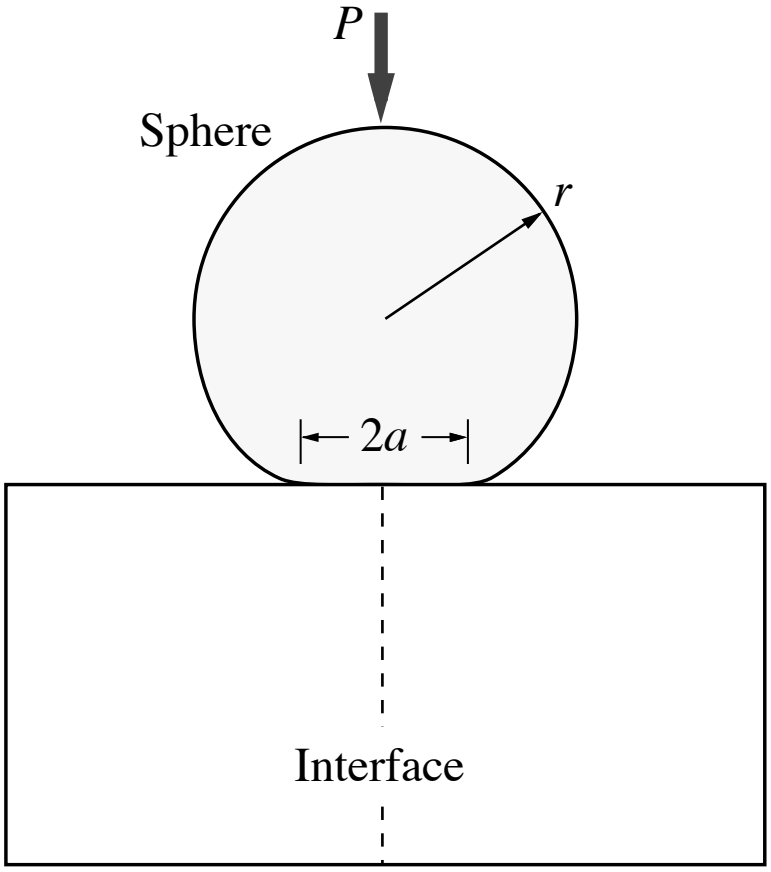

Fig. 1

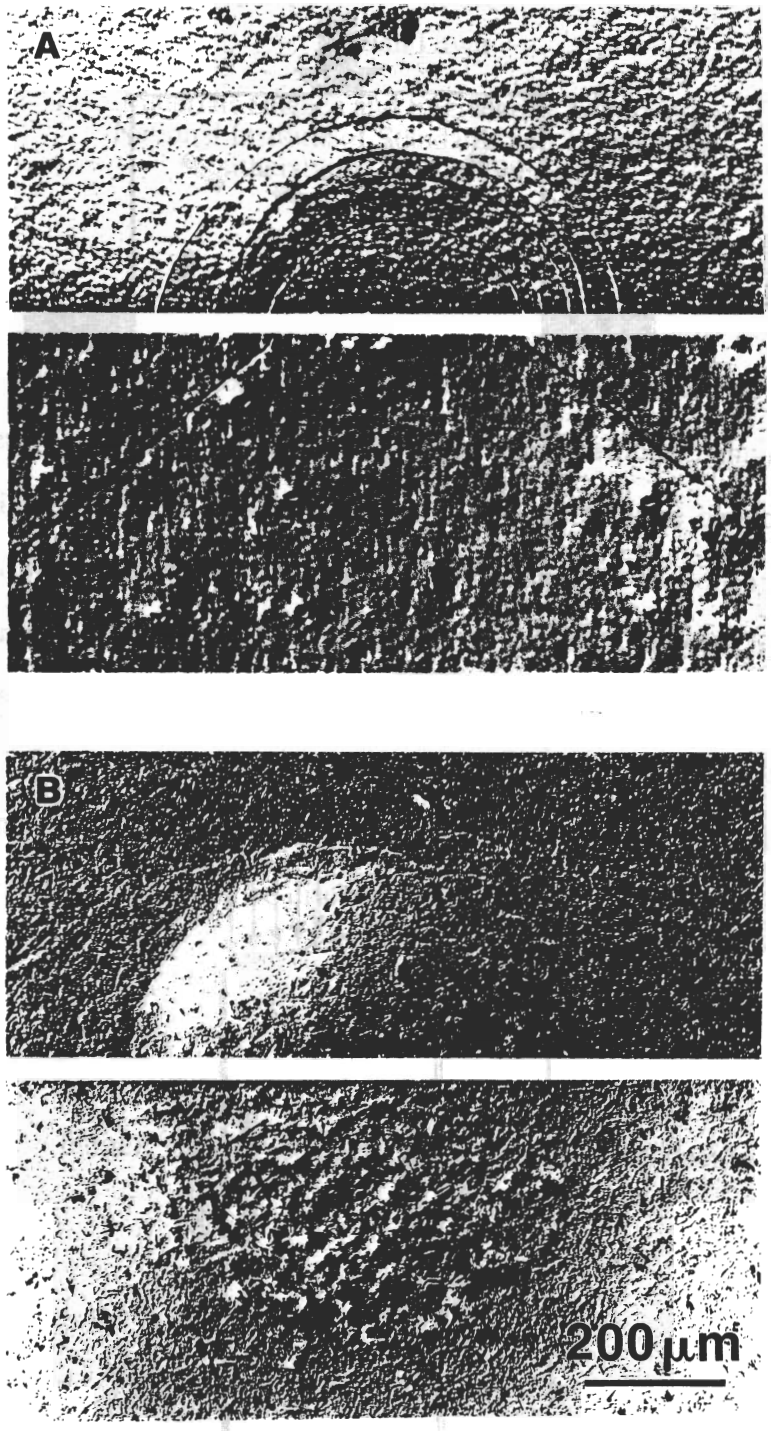

Fig. 2

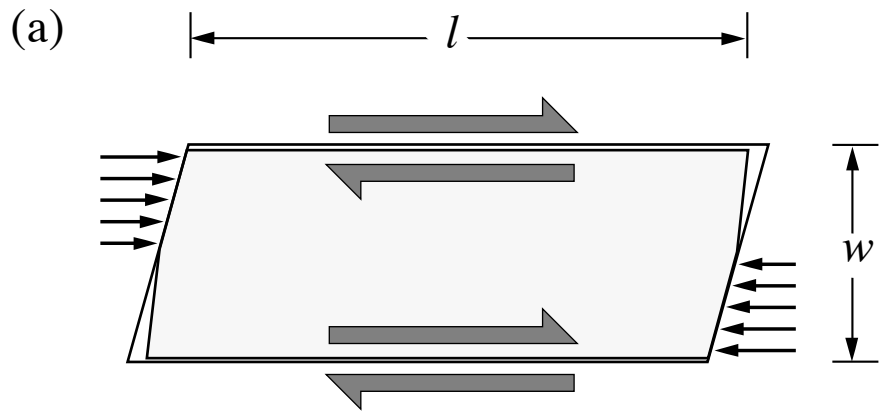

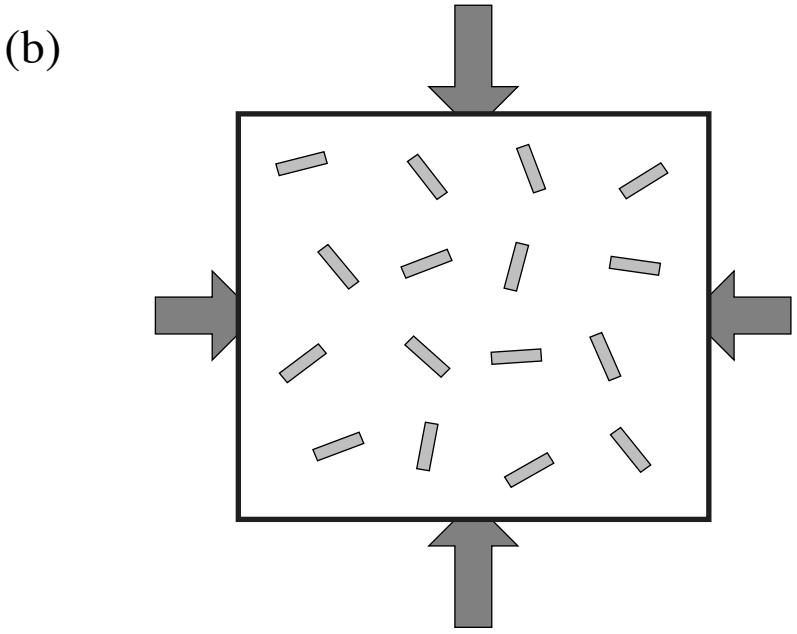

Fig. 3